

Use of brewer's residual yeast for production of bacterial nanocellulose with *Gluconacetobacter hansenii*

Gabriela Martins de Paiva^a, Letícia Fernanda de Melo^b, Fernanda Palladino Pedroso^c,
Patrícia da Luz Mesquita^a, Edson Romano Nucci^{a,d}, Igor José Boggione Santos^{a,d,*}

^a Graduate Program in Chemical Engineering, Federal University of São João del-Rei, Campus Alto Paraopeba, MG 443, km 7, 36420-000 Ouro Branco, MG, Brazil

^b Graduate Program in Bioprocess Engineering, Federal University of São João del-Rei, Campus Alto Paraopeba, MG 443, km 7, 36420-000 Ouro Branco, MG, Brazil

^c Institute of Biological Sciences, Federal University of Minas Gerais, Pres. Antônio Carlos Avenue, 6627, Pampulha, 31270-901 Belo Horizonte, MG, Brazil

^d Department of Chemistry, Biotechnology and Bioprocess Engineering, Federal University of São João del-Rei, Campus Alto Paraopeba, MG 443, km 7, 36497-899 Ouro Branco, MG, Brazil

ARTICLE INFO

Keywords:

Waste beer yeast
Hydrolysate
Fermentation
BNC
Alternative substrate
DCCR

ABSTRACT

Bacterial nanocellulose (BNC) has attained elevated interest due to its versatile structure and high resistance characteristics. Accordingly, efforts have been made in order to reduce its production costs, such as the employment of its by-products as a nutrient broth to yield the microorganism. Residual brewer's yeast is an excellent recourse, due to its high nutritional value and availability. Therefore, research which aimed to contribute to the development of a low cost, efficient and biosustainable technology for BNC production with *Gluconacetobacter hansenii* was carried out. BNC was obtained from residual brewer's yeast hydrolysate at pH 7.0 and five days of incubation at 30 °C in static culture. The hydrolysate was characterized by the amount of sugars, fatty acids, total proteins and ash content. Subsequently, BNC obtained was characterized in terms of yield, carbon conversion ratio, hydrodynamic size, crystallinity, morphology, Fourier-transform infrared spectroscopy, and surface analysis. Residual brewer's yeast hydrolysate proved to be efficient in BNC production via gluconeogenesis with consumption of alanine, threonine and glycerol, obtaining 1.9 times the yield of the chemically defined broth adopted as standard. Additionally, properties observed in the obtained BNC were equal to those obtained from conventional chemical medium. The research contributed to bacterial nanocellulose production using by-products from the brewing industry.

1. Introduction

Cellulose (C₆H₁₀O₅)_n is the most abundant biopolymer in nature, being found in all plant substances and corresponding to approximately 40 % of all available carbon reserves in these species. It is reported that approximately 1.5•10¹² tons of cellulose are produced annually, constituting one of the largest fractions of total biomass produced in the world [1]. Among the biopolymer's main characteristics, it is most notably a fibrous material, resistant, insoluble in water, biodegradable and responsible for maintaining plant cell wall structures. As a natural polymer, it retains a high-performance process with inherent advantages regarding its safety, biocompatibility, biodegradability and a versatile structure with broad possibilities for obtaining nanocomposites with different properties [2].

Besides plant cellulose, there is also bacterial nanocellulose (BNC), which is synthesized by aerobic bacteria, such as those of the genera *Gluconacetobacter*, *Agrobacterium*, *Alcaligenes*, *Pseudomonas*, *Rhizobium* or *Sarcina* and forms a kind of gelatinous, translucent film on the air-liquid interface of these microbial cultures [3]. Despite having the same structural formula, nanocellulose can be found in three forms: fibrillated nanocellulose (NFC), cellulose nanocrystals (CNC) and bacterial nanocellulose (BNC). The main differences between these types of nanocellulose are in their structure: cellulose organized in parallel bundles in the case of NFC or in crystals in the case of CNC; and in its origin: NFC is obtained from wood fibers, NCC comes from plants and other sources and NCB is produced by non-photosynthetic fermentation processes by the aforementioned bacteria. [3].

According to Jedrzejczak-Krzepkowska et al. (2016), various

* Corresponding author at: Graduate Program in Chemical Engineering, Federal University of São João del-Rei, Campus Alto Paraopeba, MG 443, km 7, 36420-000 Ouro Branco, MG, Brazil.

E-mail address: igorboggione@ufsj.edu.br (I.J.B. Santos).

<https://doi.org/10.1016/j.ijbiomac.2023.124897>

Received 18 November 2022; Received in revised form 19 April 2023; Accepted 12 May 2023

Available online 15 May 2023

0141-8130/© 2023 Elsevier B.V. All rights reserved.

bacteria strains capable of producing BNC differ in their carbon source preferences for different metabolic pathways; thus being, in most cases, glucose, glycerol, sucrose and mannitol the ones which present the highest yield [4]. In 2007, Velasco-Bedrán and López-Isunza proposed a universal model for the basic metabolism of *Gluconacetobacter* species. According to the authors, species of this genre, due to a lack thereof or low phosphofructokinase activity (PFK), are unable to synthesize pyruvate from glucose (via Embden-Myerhof-Parnas). Instead, pyruvate is obtained from acetate, glycerol or amino acids and is used to synthesize glucose through gluconeogenesis [5].

Considering BNC production, it is important to note that composition of the environment, pH and temperature are not the only factors that influence overall biopolymer performance; therefore, other factors should also be taken into account, such as form of a bioreactor, surface area and average volume of static cultures and intensity of mixing or shaking agitated fermenters/cultures [4].

Bacterial nanocellulose, despite having a molecular formula similar to plant cellulose ($C_6H_{10}O_5$)_n, possesses distinctive characteristics, such as high purity and absence of hemicellulose, pectin and lignin, which turn BNC purification into a simpler, easier and energy-efficient process when compared to plant cellulose purification. Furthermore, bacterial cellulose can be molded into different shapes during and after biosynthesis, making it a very enticing biopolymer. Besides, BNC has a high elasticity modulus, a high polymerization degree, high permeability, high porosity, excellent mechanical strength and high surface area. The latter, combined with porosity, favors its applicability as an adsorbent material [6].

However, the production of BNC is hampered by its elevated cost due to synthetic substrates employed. In order to circumvent this limitation, it is of utmost importance to carry out tests regarding utilized substrates. The recommended standard is MYP (mannitol yolk polymyxin) broth, which is high cost; hence, increasing production costs. An alternative substrate for BNC production is brewing industry waste [7].

The beer industry is one of the main economic harbors in Brazil, with production of approximately 13.3 billion liters in 2020 according to the Brazilian Beer Industry Association (CervBrasil). With such an elevated production, there is a subsequent generation of industrial waste, such as brewer's yeast. In general, yeast corresponds to between 1.5 and 3.0 kg of waste for every 100 L of beer produced [8].

Residual brewer's yeast – after fermentation – fosters from 35 to 60 % of protein dry mass, in addition to carbohydrates, minerals, lipids, enzymes and vitamins of the B complex. Because of this composition, yeast is used in animal feed formulation, in obtaining products of high nutritional value in the pharmaceutical industry and in the human diet, as well as in microorganism cultures [9–11].

Application of material waste presents itself as a viable recourse in order to improve the efficiency of BNC biosynthesis when compared to employment of monosaccharides as carbon sources; hence, doubling performance in comparison to when only monosaccharides are used [4], proving the versatile metabolism that individuals of the genus *Gluconacetobacter* have.

With high protein content of the utilized substrate, it is expected that the species *Gluconacetobacter hasenii* uses proteins for pyruvate production and subsequent glucose conversion; thus, generating energy for BNC production.

Therefore, research was carried out in order to evaluate this production through experimental designs and BNC characterization in static culture using *Gluconacetobacter hasenii* as an alternative substrate from the brewing industry – the residual yeast hydrolysate – without supplementing the substrate with any other components (no added sugar or others). Moreover, the research attempted to further evaluate the hypothesis regarding the gluconeogenesis metabolic route used by bacteria in BNC production.

2. Material and methods

2.1. Material

The strain of the bacterium *Gluconacetobacter hasenii* (ATCC 23769) was acquired from the André Tosello Tropical Culture Collection (CCT), Campinas – SP. The brewer's residual yeast was donated by the company and incubated at the Federal University of São João del-Rei, Campus Alto Paraopeba, TECDEF (Technology in Distilled and Fermented).

2.2. Methods

2.2.1. Pre-treatment and preparation of the brewer's residual yeast hydrolysate

Brewer's residual yeast was pre-treated according to the methodology described by Lin et al. (2014) [12]. Substrates were dried in an oven (Solab) at 100 °C for 48 h, crushed in a blender (Walita) and solid was subsequently resuspended at 15 % (m·v⁻¹) in distilled water. The suspension was sonicated with pointer ultrasound (Unique) at 500 W for 40 min. It was then subjected to acid hydrolysis (HCl) at 121 °C for 20 min at pH 2.0 and, next, centrifuged (Eppendorf 5920R) for 15 min at 3488g. The supernatant – a.k.a. hydrolysate – was autoclaved (Autoclave Vertical CS, Primatec Autoclaves) at 1 atm and 110 °C for 15 min and then stored at 4 °C, whilst the precipitate was properly discarded. The hydrolysate was characterized according to methodologies described in item 3.1.

2.2.2. Obtaining the inoculum

60 µL of the cryopreserved culture was added to 5.0 mL of sterile BHI (Brain Heart Infusion; Himedia) broth and incubated at 30 °C in a bacterial oven for 24 h, in static culture.

2.2.3. BNC production via static culture

The hydrolysate was employed as a substrate for bacterial growth and BNC production without any medium supplementation. Preliminary tests were carried out to monitor cell growth and sugar consumption. The brewer's residual yeast hydrolysate was used in 125 mL Erlenmeyer flasks containing 50 mL medium and incubated at 30 °C for 96 h [13]. The experiments were performed in duplicate. The samples were collected at regular intervals of 12 h and cell concentration was determined. The culture broth was centrifuged (3000 ×g for 15 min) and the supernatants were stored at –20 °C for subsequent analysis of sugars by high-performance liquid chromatography (HPLC).

After the preliminary test, in order to determine best conditions for BNC production, an experimental design was traced using Central Composite Rotatable Design – DCCR – fractionated 2² with 4 axial points and triplicate at the central point, totaling 11 trials. Variables evaluated were pH (3.4–7) and incubation time (5–20 days). BNC was obtained via aerobic batch static fermentation, in which 400 mL of hydrolysate were placed in a properly sanitized container with filtered air circulation and covered with cotton. Then, 200.0 µL of the inoculum previously activated in BHI broth were added, sustained in static culture. After cultivation, the BNC, separated from the substrate by vacuum filtration, was washed abundantly in running water, then soaked in 0.1 mol·L⁻¹ NaOH. The solution was then heated to 80 °C for 2 h on a hot plate (IKA C- MAG HS10) in order to remove all bacteria and subsequently washed thoroughly with distilled water to completely remove the alkali. Purified BNC was dried at 105 °C until reaching constant mass and then stored at 25 °C for further analysis. The same procedure was performed in order to obtain BNC using MYP broth as a culture medium. BNC production yield using residual brewer's yeast hydrolysate was observed side-to-side with the BNC production yield using the standard MYP substrate.

2.3. Analytical methods

2.3.1. Substrate characterization

2.3.1.1. Fatty acids and sugars. The total amount of sugar was quantified by DNS method. In order to identify the substances, the material was analyzed via HPLC – High-Performance Liquid Chromatography. Analyzes were carried out at the Institute of Biological Sciences of the Federal University of Minas Gerais. The column used was SUPELCOGEL C610H 6 % Crosslinked (Sigma-Aldrich) and the mobile phase was a 0.05 mol·L⁻¹ H₂SO₄ solution prepared in MilliQ® water [13].

2.3.1.2. Moisture content. 30 mL of hydrolyzed substrate were added to porcelain crucibles – which were previously dried – and weighed on an analytical balance (Shimadzu, Japan). Crucibles were placed in an oven at 105 °C until reaching constant mass. The crucible masses with the sample were documented before and after drying at 105 °C in an oven. Moisture content was determined by the difference between mass measured at the beginning and after reaching constant mass value in the oven [14].

2.3.1.3. Ash content. The sample obtained from item 2.2.4.1 was incinerated in a muffle furnace (Hipperquímica) at 550 °C until ash was obtained and, subsequently, its content was measured by the difference between its final and initial mass [14].

2.3.1.4. Protein content. The Bradford method was employed with bovine serum albumin (BSA) as the standard, within the range of 100 to 2000 mg·mL⁻¹. 10 µL of hydrolysate and 200 µL of Bradford reagent (Sigma-Aldrich) were pipetted into each well of a 96-well microplate. After 10 min, reading was performed with a microplate reader at 630 nm.

2.3.1.5. Magnetic resonance spectroscopy. In order to obtain the ¹H NMR spectrum, 20 mg of sample was extracted with a combination of 0.750 mL of a KH₂PO₄ buffer solution in D₂O (pH 6.0), containing 0.01 % (m·v⁻¹) of 3-trimethylsilyl-sodium 2,2,3,3-propionate-d₄ (TSP-d₄) as an internal reference and 0.750 mL of methanol-d₄. After being combined with solvent, the sample was vortexed for 1 min, placed in an ultrasound bath for 20 min and centrifuged at 17000 g. Then, 800 µL of supernatant was transferred to a 5 mm diameter NMR tube. ¹H NMR spectrum was obtained using a Bruker AVANCE DRX400 spectrometer at 300 K, with a spectral window of 20 ppm, many points with 65 k, averaging 32 samples, with acquisition times (AQ) and recovery (d1) of 2.0 s. For processing, a 0.3 Hz line broadening was used, prior to the Fourier transform. Phases and baselines were automatically corrected using the TopSpin 4.0.9 program and, the spectrum was calibrated by the TSP-d₄ signal at 0.00 ppm. Compound identifications were performed using Chenomx NMR Suite 9.0 (Chenomx Inc.) program, which compared the spectrum obtained with those of pure substances from the program's database.

2.3.2. Characterization of BNC

2.3.2.1. BNC yield. BNC yield was obtained by the amount of dry BNC (mg) per volume unit of substrate (mL) following Eq. (1) [7].

$$\text{Yield} = \frac{\text{Dry mass of BNC (mg)}}{\text{Volume of substrate (mL)}} \quad (1)$$

2.3.2.2. Carbon conversion ratio. The CCR was obtained by the amount of dry BNC (mg) and the amount of contained sugar (mg), according to Eq. (2) [7].

$$\text{CR} = \frac{\text{Dry mass of BNC (mg)}}{\text{Mass of contained sugar (mg)}} \cdot 100 \quad (2)$$

2.3.2.3. Particle size distribution. The BNC hydrodynamic size and polydispersity index (PDI) were obtained via dynamic light scattering. Measurements were performed at 25.0 ± 0.5 °C using Zeta Sizer S (Malvern Instrument) with an avalanche photodiode detector and correlator with no further purification. The light source was a HeNe laser of 35 mW and wavelength of 632.8 nm, linearly polarized. For intensity control, a system of crossed polarizers was used. Detection angle was fixed at 173° and measurements were correlated by the CONTIN algorithm. Optimized BNC Zeta potential was determined by laser Doppler electrophoresis.

2.3.2.4. BNC thermostability. Differential thermogravimetric analysis was performed on a DTG analyzer (DTG—60H, Shimadzu) and behavior of thermal events was performed using a Differential Scanning Calorimeter (DSC-60 Plus Model, Shimadzu). Temperature ranged from 25 to 600 °C, at a rate of 10 °C·min⁻¹ under nitrogen atmosphere with a flow rate of 50 mL·min⁻¹. Thermodynamic parameters of dehydration temperature and glass transition, mass loss and enthalpy of dehydration and degradation could then be calculated.

2.3.2.5. Crystallinity. The BNC X-ray diffraction pattern was obtained by an X-ray diffractometer (Shimadzu) with a 3 kW X-ray generator and LFF Cu anode. The radiation was CuKα of wavelength 1.54 Å. Voltage and current of the X-ray generator were 40 kV and 30 mA, respectively. Angular scan ranged from 10 to 30° with a step of 0.02° and ramp of 1°·min⁻¹.

Results obtained in the XRD analysis were used to determine the crystallinity index, according to the Segal method, shown by Eq. (3).

$$I_{CR}(\%) = \frac{I_{002} - I_{AM}}{I_{002}} \cdot 100 \quad (3)$$

where I_{CR} is the crystallinity index expressed as a percentage, I_{002} is the maximum diffraction intensity corresponding to the crystalline material and I_{AM} is the minimum diffraction intensity of the amorphous region.

2.3.2.6. Analyses of morphology and composition using Scanning Electron Microscopy (SEM). Morphological analysis of BNC was performed via Scanning Electron Microscopy (SEM, Tescan Vega3 LMU) coupled to an Energy Dispersive X-Ray (EDS) detector for qualitative elemental analysis. Air-dried BNC was fixed to a copper tip using double-conducting carbon adhesive tape and coated with platinum for 30 s. Images were obtained at 25 °C and 20 kV.

2.3.2.7. Fourier-Transform Infrared Spectroscopy (FTIR). FTIR spectra of BNC samples were obtained using the Cary 630 FTIR spectrometer (Agilent), equipped with an attenuated total reflectance (ATR) accessory. Spectra were obtained within the range of 650 to 4000 cm⁻¹, with 32 scans, at 25 °C. The spectrum was corrected at baseline and optimized.

2.3.2.8. Surface analysis. Specific surface area and porosity were determined via Brunauer-Emmet-Teller (BET) multipoint analysis in Nova Station A equipment, using nitrogen as an inert gas. Adsorption and desorption of N₂, at 77 K, were used to determine the specific surface area of the prepared material. From isotherms obtained, BET surface area and pore size distribution were calculated.

3. Results and discussion

3.1. Substrate characterization

The hydrolysate had a moisture content of 40.9 ± 0.04 % and an ash content of 6.9 ± 0.1 %. Marson et al. (2019) characterized the residual brewer's yeast after the Brauzy hydrolysis and obtained an ash content of

8.9 ± 0.0 % [15]. Studies claim that *Saccharomyces cerevisiae* has a moisture content between 70 % and 80 % [16]; however, high-temperature heat treatments and autoclaving processes may have reduced this content in hydrolysate. Hydrolysate presented 0.26 g·L⁻¹ of protein. Regarding sugar content, the hydrolysate obtained a value of 15.5 g·L⁻¹, determined via DNS method. Sugars identified by HPLC in the residual brewer's yeast hydrolysate were trehalose, glucose, fructose, mannose, and ribose. Ethanol, glycerol and acetic acid were also found in the material.

In Fig. 1, through Magnetic Resonance Spectroscopy, it is possible to identify the region from δ 1.0–2.0, two doublets: one in δ 1.48 [d; 7.3 (Hz)] and another in δ 1.32 [d; 6.8 (Hz)], indicating presence of alanine and threonine amino acids, respectively. Coupled with total reducing sugar analysis, it can be noted that there are not enough carbohydrates in the hydrolysate for the bacterium *Gluconacetobacter hansenii* to rely solely on this source of energy and perform glycolysis. According to Hutchens et al. (2007), for BNC synthesis to occur, glucose is oxidized by membrane-bound glucose dehydrogenase, which provides electrons to metabolic processes. When there is inhibition of glucose oxidation due to the presence of ethanol or glycerol, an increase in BNC production yield is observed, because bacteria of the *Gluconacetobacter* genus oxidize alcohol into acetic acid in order to obtain electrons and, thus, begin synthesizing BNC through alternative metabolic pathways to attain glycolysis. One of the alternative pathways is gluconeogenesis, in which glucose is synthesized from substances other than carbohydrates such as amino acids, lactate, glycerol, and propionic acid, for instance [17]. Therefore, it is suggested that the metabolic route chosen by the

bacterium *Gluconacetobacter hansenii* for BNC production is gluconeogenesis, since brewer's yeast hydrolysate is low in carbohydrates and, contrastingly, rich in gluconeogenic amino acids, such as alanine and threonine.

3.2. BNC Characterization

3.2.1. Obtaining BNC

BNC was obtained via aerobic batch static fermentation, in which 400 mL of hydrolysate were placed in a properly sanitized container with filtered air circulation and covered with cotton. Then, 200.0 μL of the inoculum previously activated in BHI broth were added, sustained in static culture, as aforementioned. The highest BNC yield was obtained with 5 days of incubation and a pH of 7.0 for the hydrolysate, obtaining a mass 1.9 times greater than when using the chemically defined broth, which is conventionally adopted (Table S1). Obtained results are in accordance with data reached by Lin et al. (2014), who used residual brewer's yeast hydrolysate treated with a combination of ultrasound and acid hydrolysis as a nutrient source for *Gluconacetobacter xylinus* bacterium to produce BNC via static culture and obtained a yield equivalent to twice the yield obtained when the traditional chemical medium was employed, as previously stated. However, it is important to emphasize that the strain used by Lin et al. (2014) is different from the one currently being described. Lin et al. (2014) used *Gluconacetobacter xylinus* while this research used *Gluconacetobacter hansenii*. Despite belonging to the same genus, bacteria may have different nutritional demands; consequently, producing BNC through different metabolic

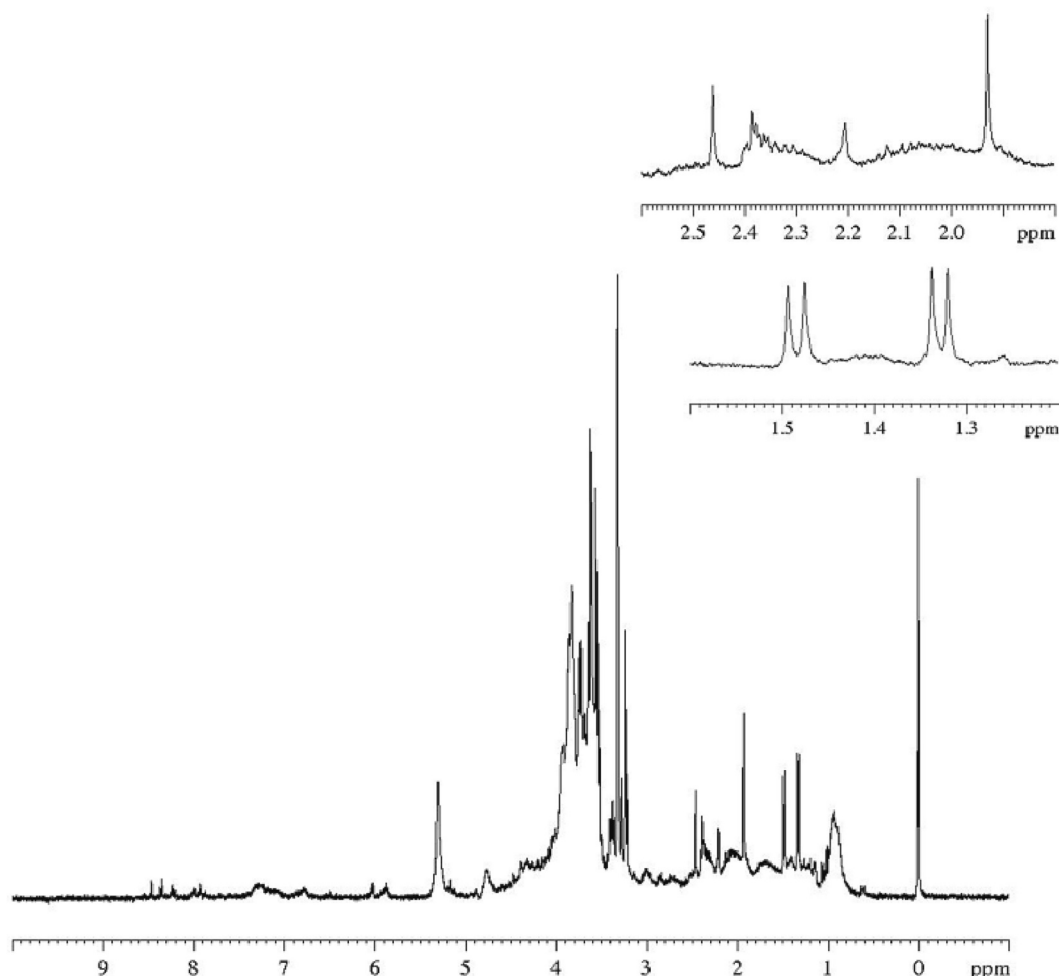


Fig. 1. ¹H NMR spectrum obtained from the brewer's residual yeast hydrolysate.

routes. Lin et al. (2014) compare different types of pretreatments so that the highest possible production of nanocellulose occurs. In the current research, the two best pretreatments chosen by Lin et al. (2014) were used concomitantly in order to improve BNC production yield [12].

Table 1 shows fermentation results for *Gluconacetobacter hansenii* bacterium under the best conditions obtained, such as cell growth and consumption of trehalose and glycerol, reversed in the intensity of the chromatogram peaks. From data in the Table 1, it can be concluded that there is no consumption of sugar or glycerol by the bacteria during fermentation, which corroborates that the metabolic pathway chosen for BNC synthesis is gluconeogenesis. E. Velasco-Bedran and López-Isunza (2007) discussed the metabolism of species from the *Gluconacetobacter* genus and concluded that acetic acid can be used as a substrate and synthesized as a product, corroborating results of HPLC analysis and the fact that the species did not consume sugars. Furthermore, according to Velasco-Bedran and López-Isunza (2007), the presence of ethanol, also evidenced by the HPLC analysis of the residual brewer's yeast hydrolysate, triggers dissimilation of the compound and initiates production of pyruvate via gluconeogenesis. Henceforth, an assumption that the metabolic route chosen by the bacterium was gluconeogenesis was based on the consumption of the gluconeogenic amino acids alanine and threonine and glycerol, which were used to then form the glucose necessary for bacteria to subsist in the medium [5]. Presence of amino acids can be verified in Fig. 1, while negligible consumption of glycerol and trehalose can be verified in Table 1. Therefore, it can be inferred that there was consumption of gluconeogenic amino acids instead of glycerol and sugars available in the medium. Thus, it was not necessary to add any kind of sugar to the medium.

3.2.2. BNC yield

Twelve batches were prepared and the average yield obtained was 13.1 ± 0.4 mg/mL. According to Lin et al. (2014), BNC production is a process that generates low yield; ergo, expensive. Additionally, according to the author, in order to minimize costs, industrial residues are studied so that they may be employed as energy sources for the bacterium *Gluconacetobacter hansenii*; however, these residues still need to undergo pre-treatments, since the bacterium cannot metabolize polysaccharides for BNC production [12].

Lin et al. (2014) observed that in order to obtain higher yields, it is necessary to add some extra nutrients to the nutrient broth obtained through the hydrolysis of brewer's residual yeast [12]. For instance, Hong and Qiu (2008) obtained an increase in BNC production with addition of Ca^{2+} introduced into the medium of konjac powder hydrolysates [18], Gomes et al. (2013) increased BNC production with addition of nitrogen and phosphate source supplements in hydrolysates of residues from olive production [19], Ha et al. (2008) improved BNC

Table 1

Yield of BNC produced in a static culture of *Gluconacetobacter hansenii* in the presence of residual brewer's yeast hydrolysate under maximum yield conditions.

Time (hours)	Cells (optical density)	Trehalose (peak intensity)	Trehalose concentration	Glycerol (peak intensity)	Glycerol concentration
		(TR = 9.77 min)	(g/L)	(TR = 15.89 min)	(g/L)
0	0.906 ± 0.021	131,721 $\pm 0,0$	$0.49 \pm 0,0$	$27,239 \pm 0,0$	$0.65 \pm 0,0$
24	1.461 ± 0.085	141,938 $\pm 0,0$	$0.53 \pm 0,0$	$28,837 \pm 0,0$	$0.69 \pm 0,0$
48	1.521 ± 0.021	140,245 $\pm 0,0$	$0.52 \pm 0,0$	$26,125 \pm 0,0$	$0.62 \pm 0,0$
72	1.634 ± 0.011	149,220 $\pm 0,0$	$0.56 \pm 0,0$	$26,678 \pm 0,0$	$0.63 \pm 0,0$
96	1.656 ± 0.085	135,124 $\pm 0,0$	$0.49 \pm 0,0$	$26,124 \pm 0,0$	$0.62 \pm 0,0$

yield with addition of glucose to hydrolyzed brewer's yeast residues as a nutritional supplement [20]. No extra nutrients were added in the current research.

3.2.3. Carbon conversion ratio

Carbon conversion ratio expresses the carbon fraction of a heterotrophic substrate that is incorporated into biomass, as shown through Eq. (2). The ratio between the amount of BNC obtained and the amount of sugar present in the culture medium was 1.8 %. As for the MYP broth, the value was 0.2 %.

This result is corroborated by the higher production which occurs in the hydrolysate of residual brewer's yeast. Furthermore, according to Hutchens et al. (2007), MYP broth is recommended for BNC production through bacteria from the *Gluconacetobacter* genus on account of it being sugar alcohol, which provides electrons for the bacteria's metabolism, stimulating a higher BNC yield when compared to media in which only glucose is used as a carbon source [17]. Therefore, it is suggested that, due to the residual brewer's yeast hydrolysate having a greater amount of alcohol, there is a greater stimulus acting upon metabolism; consequently, leading to a greater carbon conversion ratio.

3.2.4. Particle size distribution

Nanocellulose presented an average hydrodynamic size of 66.9 ± 15.3 nm. Regarding the polydispersity index, nanocellulose presented 0.4 ± 0.0 , indicating a relatively low polydispersity due to the fact that, for natural polymers, PDI values lower than 0.4 are considered low while values greater than 0.4 are connected to high polydispersity nanoparticles [21]. The BNC Zeta potential was -18.4 ± 3.5 mV, at pH 7.0. Carboxylate groups present on BNC surface may be responsible for the negative value [22].

3.2.5. BNC thermostability

TG analysis of BNC indicated a continuous total mass loss of 50.2 %, with a temperature increase from 25 °C to 600 °C, which can be divided into three distinct sections: from 25 °C to around 180 °C, with a loss of about 17.3 % mass; from 180 °C to 560 °C, with a mass loss of approximately 32.1 % and lastly from 560 °C to 600 °C, with a mass loss of 0.9 %, as shown in Fig. 2. BNC thermal degradation started at a temperature of approximately 120 °C, with the endothermic peak reaching its end as shown by the DSC, indicating water loss. Thus, events before this temperature can be correlated to BNC dehydration.

The glass transition temperature (T_g) of BNC is between 120 °C and 156 °C, differing from values commonly found in literature. According to the literature, the glass transition temperature, for dry and isolated cellulose, is between 200 °C and 250 °C. However, according to Hosseini et al. (2018), this temperature range does not refer to the T_g of the cellulose, but to its degradation temperature. The T_g of highly crystalline macromolecules is difficult to determine [23]. The bacterium used to produce nanocellulose, *Gluconacetobacter hansenii*, is a species of acetic acid bacteria; that is, it oxidizes sugars or ethanol and produces acetic acid during fermentation [24]. Therefore, it is suggested that the glass transition temperature of the BNC produced in this work is in the temperature range of 120 °C and 156 °C, followed by the other phases of depolymerization and total degradation of the sample. The second stage of the analysis – which represented the greatest mass loss – is responsible for depolymerization and decomposition of glycosyl units. As indicated by the graph, degradation via presence of exothermic peaks is characteristic of degradation reactions. The third and final step was represented by the graph part which tends to linearize, concerning formation of a carbonized residue [25–27].

3.2.6. Crystallinity

According to Eq. (3), the I_{CR} for the BNC obtained was 76.3 % and for its calculation, values regarding the peak close to 34° for the crystalline region and 36° for the amorphous region were used. Treatments into which cellulose samples are subjected can significantly affect their

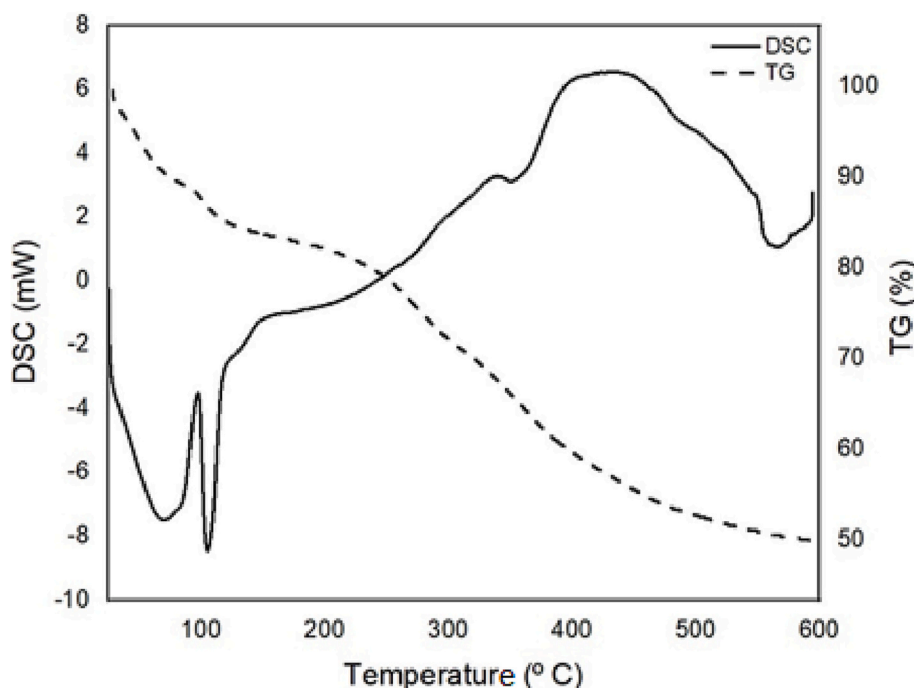


Fig. 2. BNC thermogram, in N_2 gas atmosphere.

degree of crystallinity [28]. When a treatment is carried out with NaOH, there is BNC mercerization, where crystallites composed of cellulose chains in a parallel orientation incorporate hydrated sodium and hydroxide ions, which can reduce crystallinity and also form cellulose II, a product of the neutralization reaction of native cellulose [29]. This change is irreversible and usually accompanied by a decrease in crystallinity. Therefore, it is suggested that BNC mercerization might have occurred after washing it with NaOH during the purification process.

Mercerized cellulose presents crystallinity peaks close to 25° , while the amorphous region is closer to around 30° [29], not far from what is shown in Fig. 3. However, crystallinity indexes were obtained for eight samples of nanocellulose within a range of 70.3 to 75.8 %, using the Segal method [30–32].

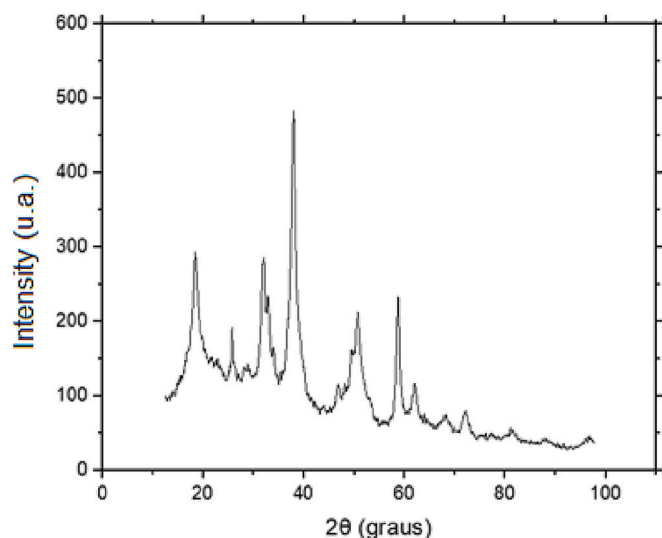


Fig. 3. X-ray diffractograms of the BNC sample obtained via residual brewer's yeast hydrolysate.

3.2.7. Analyses of morphology and composition using Scanning Electron Microscopy (SEM)

BNC morphological analysis was performed in three steps, in which images were zoomed in 350, 502 and 1000 \times , as shown in Fig. 4. BNC morphology consists of an irregular surface characterized by numerous interlaced and asymmetrical nodes. Results also indicate that BNC has a rough structure, which can be attributed to its network of unevenly dispersed and randomly overlapping fibrils [33]. Arrows indicate possible fibrils. According to Mohammadkazemi (2017), BNC's surface roughness can be attributed to its high surface area and crystallinity [34]. The intertwined nature and porosity of BNC greatly increase swelling, which allows the adsorption and absorption of several substances by this material [33].

According to the EDS analysis, as shown in Fig. 5, it is possible to conclude that the composition of the BNC is characterized by the majority presence of the following elements such as carbon (C) and oxygen (O). Other compounds in smaller amounts are present, such as: sodium (Na), magnesium (Mg), silicon (Si), phosphorus (P), sulfur (S), potassium (K) and calcium (Ca). Results show that BNC contains typical elements (C and O) that make up the building blocks of cellulose – $(C_6H_{10}O_5)_n$. However, the low concentration of other metals present in BNC occurs due to the contact of these metals during the process of obtaining or treating the sample which may affect the presence, concentration and distribution of metals or inorganics elements in bacterial cellulosic materials [33]. Presence of Na in BNC composition is due to the treatment and processing of BNC in the presence of NaOH, which is used for pH adjustment, as well as for washing obtained BNC. Other metals come from processing BNC in the yeast hydrolysate [33]. According to Chen et al. (2014), it is possible to observe C, N, O, P, K, Mg and S on the surface of *Saccharomyces cerevisiae* yeast via EDS [35]. Can et al. (2008) found K, Ca, Mg, and Na when they analyzed the yeast surface [36]. Therefore, as in the case of NaOH, there may have been elemental cross-transfers, which occur due to the contact BNC goes through during its processing or treatment with the metals found in EDS analysis.

3.2.8. Fourier-Transform Infrared Spectroscopy (FTIR)

From the analysis of Fig. 6, it is possible to determine the main

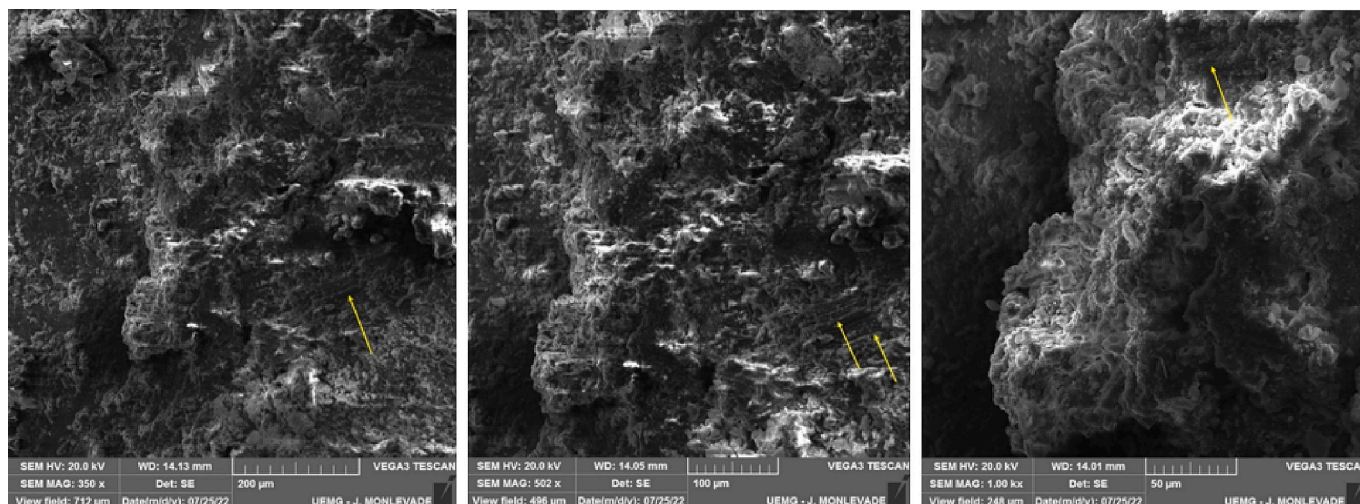


Fig. 4. BNC images obtained by SEM and approximated 350, 502 and 1000 times respectively.

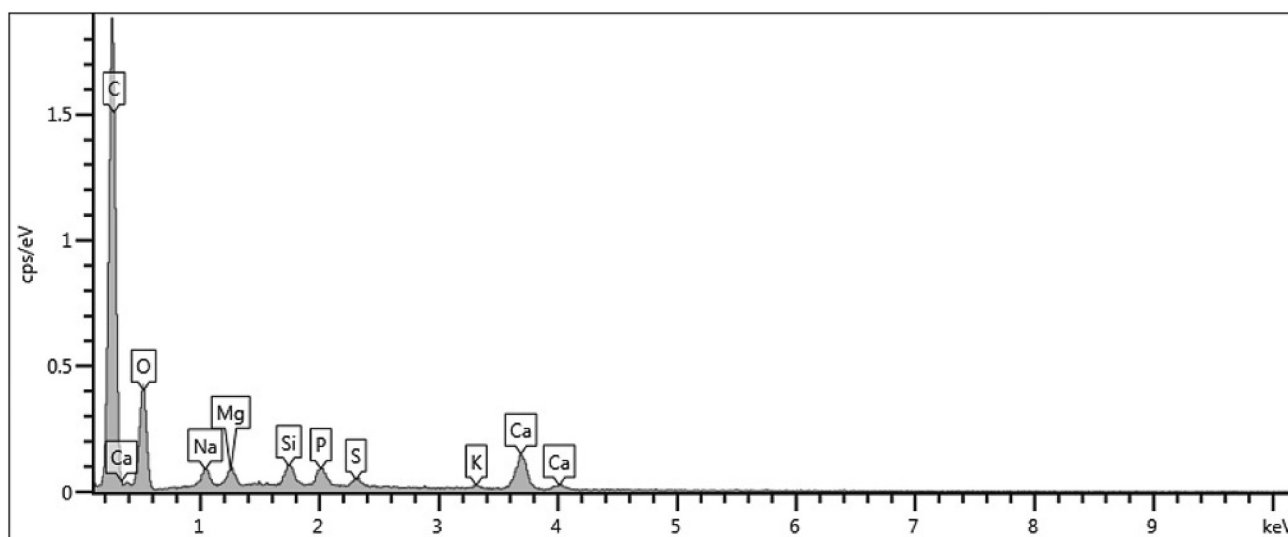


Fig. 5. BNC EDS spectrum.

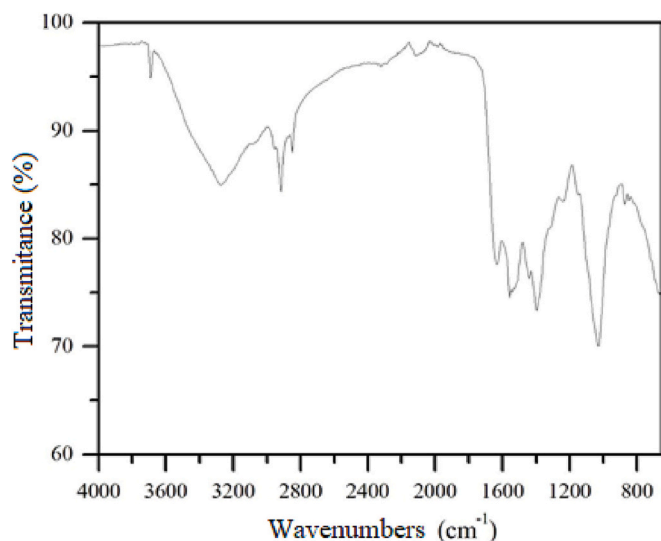


Fig. 6. FTIR spectrum of BNC obtained via residual brewer's yeast hydrolysate.

functional group peaks for the components of the material and intra-molecular hydrogen bonds typical of a polysaccharide. Hydrogen bonding of hydroxyl groups was characterized by the absorption band in the wavelength region between 3600 and 3100 cm^{-1} . Peaks observed in the wavelength region between 2940 and 2860 cm^{-1} represent C—H bonds of the polysaccharide [37]. Thus, the region comprising a wavelength between 1200 and 800 cm^{-1} pertains to monosaccharides [38]. Peaks observed at wavelengths between 1637 and 1456 cm^{-1} indicate presence of free carboxyl groups [39]. FTIR spectrum of BNC includes peaks in the regions between wavelengths of 3600 and 3100 cm^{-1} , as well as in the region between 1200 and 800 cm^{-1} , corresponding to glucose, which has a large number of hydrogen bonds [40,41].

Henceforth, cellulose molecules are deposited in microfibrils in which there is an extensive amount of hydrogen bonds between cellulose chains, corroborating images obtained via SEM and producing a strong crystalline structure; thus, corroborating data obtained via XRD [42].

3.2.9. Surface analysis

The isotherm resulting from adsorption between N_2 and BNC in the BET analysis shown in Fig. 7 is type II, according to Brunauer, Emmet, and Teller (1938), which suggests that the adsorbent-adsorbent

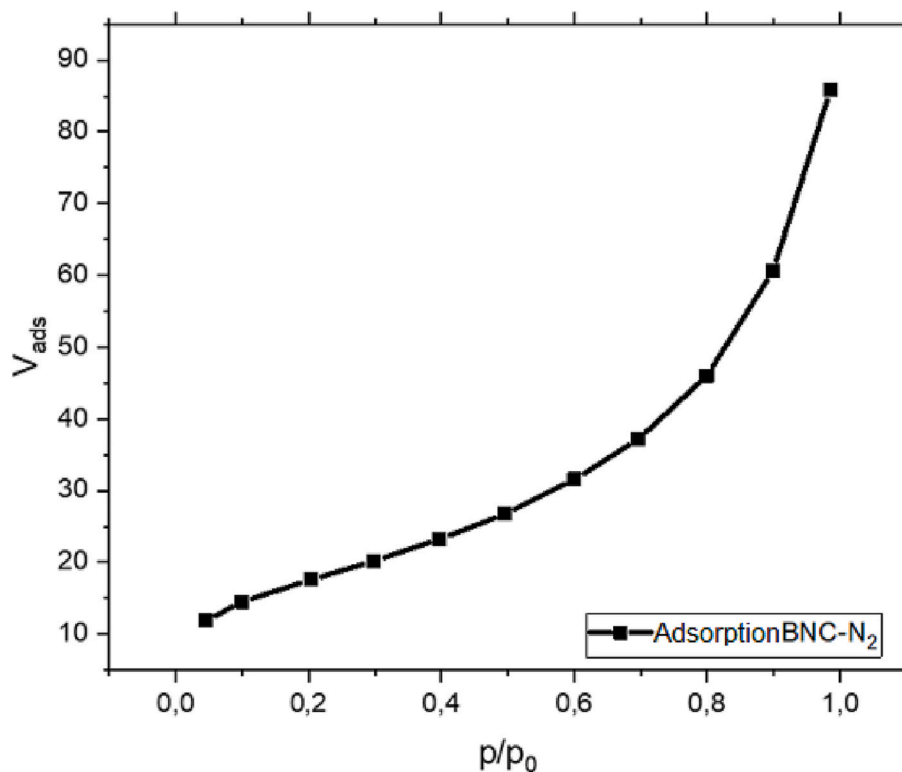


Fig. 7. BNC-N₂ adsorption isotherm.

interaction is weak and indicates the occurrence of multilayer adsorption without the necessity of completely forming the first layer [43]. Fig. 8 shows the adsorption-desorption of N₂ on BNC at 77 K. The behavior of the amount of gas adsorbed versus the value of P/P_0 depends on the material porous characteristics; hence, according to IUPAC, adsorption-desorption of N₂ in BNC is type IVa. These isotherms describe

adsorption processes in which there is the formation of monolayers and/or multilayers, until formation of regions on which there is a sudden increase in the amount of gas adsorbed by the material. After the formation of these regions, saturation occurs, indicating that all pores have been filled and the material is no longer able to adsorb gas. Furthermore, type IV isotherms can differentiate into IVa and IVb, which are

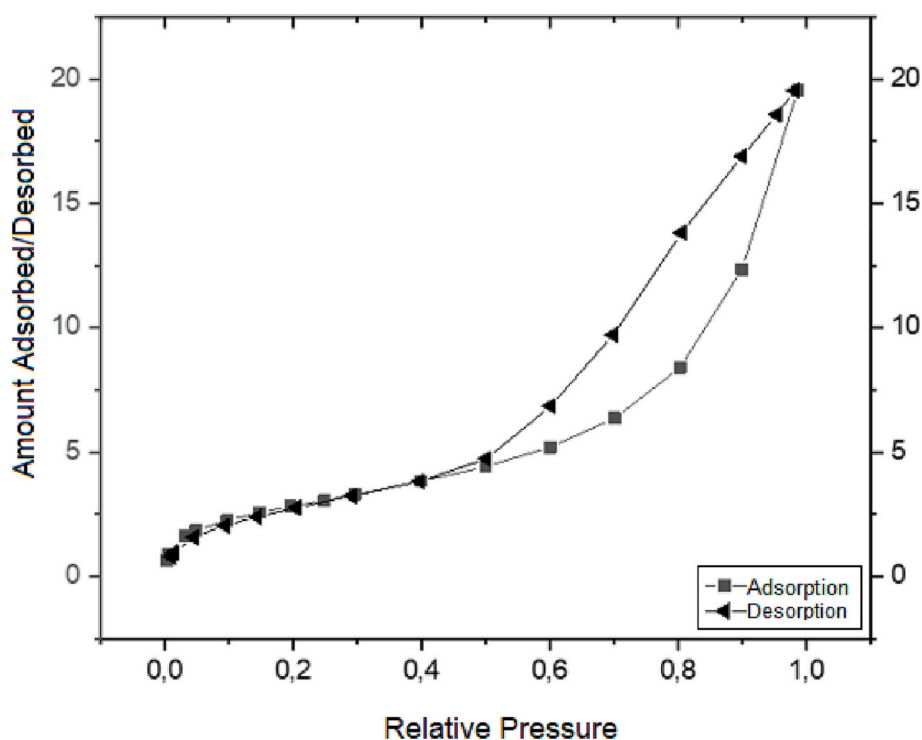


Fig. 8. Volumetric adsorption-desorption of N₂ in BNC.

hysteresis of the material initial behavior [44].

When interactions between the adsorbent and the adsorbate are weak, yet there are micropores or mesopores in the material, adsorption at low relative pressures is small. However, there may be a certain pressure which leads to sudden increase in the adsorption of gases due to pore filling. In this case, it is difficult to determine the amount of gas needed to form the monolayer [44].

Hysteresis is an element of isotherms which originate from adsorption processes that are not completely reversible; that is, when it is difficult for the adsorbate to detach from the adsorbent during the desorption process. According to IUPAC, five types of possible hysteresis differ from each other due to the pressure range in which they occur, as well as their shape. The hysteresis presented by the adsorption/desorption of N₂ in BNC is of type IIB and occurs in intervals of high relative pressure, being originated due to the formation of menisci; that is, regions where there is a sudden increase in the amount of gas adsorbed by the material. The wide range in which hysteresis is present suggests that the exit of the adsorbate from the interior of the matrix is hampered on account of the large interconnection within the porous network [44].

In addition to the isotherm obtained, it was also possible to obtain data regarding BNC pore size, which is presented in Table 2. The high specific area and the negative Zeta potential values make BNC a material of interest for the adsorption of cations.

The differentiation for obtained BNC types is correlated to the form of the culture, whether it be static or agitated, ultimately producing either the nanocellulose film or crystals. Furthermore, supplementation of culture media with plant residues affected the cellulose structure in many cases [4]. For instance, the nanostructure of the biopolymer derived from a rice husk-based medium, which contained lignin, hemicelluloses and mineral salts, was different from the BC synthesized in the glucose-based reference medium and was considered a potential new nanostructured drug transporter [45] with a tensile strength 79 % higher than the BNC reference [18].

4. Conclusions

The current research proves the efficiency of using the residual hydrolysate of brewer's yeast for the production of bacterial nanocellulose via static cultivation of the bacterium *Gluconacetobacter hansenii*, previously prepared by sonication and acid hydrolysis, whose best yield was obtained in broth with pH 7.0 and 5 days of incubation in static culture. The metabolic route chosen by the bacterium was gluconeogenesis, as evidenced by the consumption of the amino acids alanine and threonine, and glycerol. The average hydrodynamic size obtained was 66.9 ± 15.3 nm and the polydispersity index was 0.4 ± 0.0 . The zeta potential presented by the BNC, at pH 7.0, was -18.4 ± 3.4 mV. BNC thermal degradation temperature was approximately 170 °C. Other characterizations prove the composition of bacterial nanocellulose is similar to vegetable cellulose. Thus, results suggest an economically and environmentally promising form of producing BNC.

Supplementary data to this article can be found online at <https://doi.org/10.1016/j.ijbiomac.2023.124897>.

CRedit authorship contribution statement

Igor José Boggione Santos: conceptualization, methodology, investigation, and writing. **Gabriela Martins de Paiva:** investigation, writing, and data curation. **Letícia Fernanda de Melo:** investigation. **Fernanda Palladino Pedroso:** investigation and data curation. **Patrícia da Luz Mesquita:** conceptualization and methodology. **Edson Romano Nucci:** data curation.

Declaration of competing interest

The authors declare that they have no known competing financial

Table 2

Evaluation of BNC surface area and porosity.

	Surface area (m ² ·g ⁻¹)	Average diameter (Å)	Total pore volume (cm ³ ·g ⁻¹)
BNC	61.575	16.200	20.174

interests or personal relationships that could have appeared to influence the work reported in this paper.

Data availability

Data will be made available on request.

Acknowledgements

The authors would like to thank the FAPEMIG for the financial support via graduate scholarship (13717-22) and UFOP CiPharma multiuser Laboratory for measurements with the Nano Zetasizer, via the project "Asymmetric Flow Field Flow Fractionation" (FAPEMIG CDS – APQ 01510-14).

References

- [1] D. Klemm, B. Heublein, H.P. Fink, A. Bohn, Cellulose: fascinating biopolymer and sustainable raw material, *Angew. Chem. Int. Ed.* 44 (2005), <https://doi.org/10.1002/anie.200460587>.
- [2] C. Zinge, B. Kandasubramanian, Nanocellulose based biodegradable polymers, *Eur. Polym. J.* 133 (2020), <https://doi.org/10.1016/j.eurpolymj.2020.109758>.
- [3] M.W. Ullah, S. Manan, S.J. Kiprono, M. Ul-Islam, G. Yang, Synthesis, structure, and properties of bacterial cellulose, in: *Bacterial Nanocellulose: From Fundamentals to Advanced Materials*, 2019, <https://doi.org/10.1002/9783527807437.ch4>.
- [4] M. Jedrzejczak-Krzepkowska, K. Kubiak, K. Ludwicka, S. Bielecki, Bacterial Nanocellulose synthesis, recent findings, in: *Bacterial Nanocellulose*, Elsevier, 2016, pp. 19–46, <https://doi.org/10.1016/B978-0-444-63458-0.00002-0>.
- [5] H. Velasco-Bedrán, F. López-Isunza, The unified metabolism of Gluconacetobacter entanii in continuous and batch processes, *Process Biochem.* 42 (2007), <https://doi.org/10.1016/j.procbio.2007.05.017>.
- [6] N. Muhd Julkapli, S. Bagheri, Nanocellulose as a green and sustainable emerging material in energy applications: a review, *Polym. Adv. Technol.* 28 (2017), <https://doi.org/10.1002/pat.4074>.
- [7] A. Basu, S.V. Vadanam, S. Lim, Rational design of a scalable bioprocess platform for bacterial cellulose production, *Carbohydr. Polym.* 207 (2019) 684–693, <https://doi.org/10.1016/j.carbpol.2018.10.085>.
- [8] S. Aliyu, M. Bala, Brewer's spent grain: a review of its potentials and applications, *Afr. J. Biotechnol.* 10 (2011) 324–331.
- [9] I.M.P.L.V.O. Ferreira, O. Pinho, E. Vieira, J.G. Távora, Brewer's *Saccharomyces* yeast biomass: characteristics and potential applications, *Trends Food Sci. Technol.* 21 (2010) 77–84, <https://doi.org/10.1016/j.tifs.2009.10.008>.
- [10] M.-J. In, D.C. Kim, H.J. Chae, Downstream process for the production of yeast extract using brewer's yeast cells, *Biotechnol. Bioprocess Eng.* 10 (2005) 85, <https://doi.org/10.1007/BF02931188>.
- [11] D.E. Briggs, P.A. Brookes, R. Stevens, C.A. Boulton, *Brewing: Science and Practice*, Elsevier, 2004.
- [12] D. Lin, P. Lopez-Sanchez, R. Li, Z. Li, Production of bacterial cellulose by *Gluconacetobacter hansenii* CGMCC 3917 using only waste beer yeast as nutrient source, *Bioresour. Technol.* 151 (2014) 113–119, <https://doi.org/10.1016/j.biortech.2013.10.052>.
- [13] F. Palladino, R.C.L.B. Rodrigues, R.M. Cadete, K.O. Barros, C.A. Rosa, Novel potential yeast strains for the biotechnological production of xylitol from sugarcane bagasse, *Biofuels Bioprod. Biorefin.* 15 (2021), <https://doi.org/10.1002/bbb.2196>.
- [14] J.W. Latimer, *Official Methods of Analysis of AOAC International, Association of Official Analytical Chemists*, 2012.
- [15] G.V. Marson, M.T. da C. Machado, R.J.S. de Castro, M.D. Hubinger, Sequential hydrolysis of spent brewer's yeast improved its physico-chemical characteristics and antioxidant properties: a strategy to transform waste into added-value biomolecules, *Process Biochem.* 84 (2019) 91–102, <https://doi.org/10.1016/j.procbio.2019.06.018>.
- [16] T.R. dos Santos Mathias, V.M.F. Alexandre, M.C. Cammarota, P.P.M. de Mello, E.F. C. Sêrvulo, Characterization and determination of brewer's solid wastes composition, *J. Inst. Brew.* 121 (2015), <https://doi.org/10.1002/jib.229>.
- [17] S.A. Hutchens, R.V. León, H.M. O'Neill, B.R. Evans, Statistical analysis of optimal culture conditions for *Gluconacetobacter hansenii* cellulose production, *Lett. Appl. Microbiol.* 44 (2007), <https://doi.org/10.1111/j.1472-765X.2006.02055.x>.
- [18] F. Hong, K. Qiu, An alternative carbon source from konjac powder for enhancing production of bacterial cellulose in static cultures by a model strain *Acetobacter acetii* subsp. *xylanus* ATCC 23770, *Carbohydr. Polym.* 72 (2008), <https://doi.org/10.1016/j.carbpol.2007.09.015>.

- [19] F.P. Gomes, N.H.C.S. Silva, E. Trovatti, L.S. Serafim, M.F. Duarte, A.J.D. Silvestre, C.P. Neto, C.S.R. Freire, Production of bacterial cellulose by *Gluconacetobacter sacchari* using dry olive mill residue, *Biomass Bioenergy* 55 (2013) 205–211, <https://doi.org/10.1016/j.biombioe.2013.02.004>.
- [20] J.H. Ha, O. Shehzad, S. Khan, S.Y. Lee, J.W. Park, T. Khan, J.K. Park, Production of bacterial cellulose by a static cultivation using the waste from beer culture broth, *Korean J. Chem. Eng.* 25 (2008), <https://doi.org/10.1007/s11814-008-0134-y>.
- [21] D.A. Madalena, Ó.L. Ramos, R.N. Pereira, A.I. Bourbon, A.C. Pinheiro, F. X. Malcata, J.A. Teixeira, A.A. Vicente, In vitro digestion and stability assessment of β -lactoglobulin/riboflavin nanostructures, *Food Hydrocoll.* 58 (2016) 89–97, <https://doi.org/10.1016/j.foodhyd.2016.02.015>.
- [22] K. Uetani, H. Yano, Nanofibrillation of wood pulp using a high-speed blender, *Biomacromolecules* 12 (2011), <https://doi.org/10.1021/bm101103p>.
- [23] H. Hosseini, M. Kokabi, S.M. Mousavi, Dynamic mechanical properties of bacterial cellulose nanofibres, *Iran. Polym. J.* 27 (2018), <https://doi.org/10.1007/s13726-018-0621-x>.
- [24] P. Raspor, D. Goranović, Biotechnological applications of acetic acid bacteria, *Crit. Rev. Biotechnol.* 28 (2008), <https://doi.org/10.1080/07388550802046749>.
- [25] S. Torgbo, P. Sukyai, Biodegradation and thermal stability of bacterial cellulose as biomaterial: the relevance in biomedical applications, *Polym. Degrad. Stab.* 179 (2020), <https://doi.org/10.1016/j.polymdegradstab.2020.109232>.
- [26] J. George, K.V. Ramana, A.S. Bawa, Siddaramaiah, bacterial cellulose nanocrystals exhibiting high thermal stability and their polymer nanocomposites, *Int. J. Biol. Macromol.* 48 (2011) 50–57, <https://doi.org/10.1016/j.ijbiomac.2010.09.013>.
- [27] Maren Roman, William T. Winter, Effect of sulfate groups from sulfuric acid hydrolysis on the thermal degradation behavior of bacterial cellulose, *Biomacromolecules* 5 (2004) 1671–1677.
- [28] M.J. Taherzadeh, K. Karimi, Pretreatment of lignocellulosic wastes to improve ethanol and biogas production: a review, *Int. J. Mol. Sci.* 9 (2008), <https://doi.org/10.3390/ijms9091621>.
- [29] P. Zugenmaier, Conformation and packing of various crystalline cellulose fibers, *Prog. Polym. Sci.* 26 (2001) 1341–1417, [https://doi.org/10.1016/S0079-6700\(01\)00019-3](https://doi.org/10.1016/S0079-6700(01)00019-3).
- [30] K. Przybysz Buzala, H. Kalinowska, P. Przybysz, E. Malachowska, Conversion of various types of lignocellulosic biomass to fermentable sugars using kraft pulping and enzymatic hydrolysis, *Wood Sci. Technol.* 51 (2017), <https://doi.org/10.1007/s00226-017-0916-7>.
- [31] L.C. Viana, G.I.B. de Muñoz, W.L.E. Magalhães, A.S. de Andrade, S. Nisgoski, D. C. Potulski, Nanostructured films produced from the bleached *Pinus* sp. kraft pulp, *Floresta e Ambiente* 26 (2019), <https://doi.org/10.1590/2179-8087.019115>.
- [32] R.S.A. Ribeiro, N. Bojorge, N. Pereira, Statistical analysis of the crystallinity index of nanocellulose produced from Kraft pulp via controlled enzymatic hydrolysis, *Biotechnol. Appl. Biochem.* 67 (2020), <https://doi.org/10.1002/bab.1873>.
- [33] M. Abba, Z. Ibrahim, C.S. Chong, N.A. Zawawi, M.R.A. Kadir, A.H.M. Yusof, S.I. A. Razak, Transdermal delivery of crocin using bacterial nanocellulose membrane, *Fibers Polym.* 20 (2019) 2025–2031, <https://doi.org/10.1007/s12221-019-9076-8>.
- [34] Faranak Mohammadkazemi, Surface properties of bacterial nanocellulose using spectroscopic methods and X-ray diffraction, *Am. J. Appl. Ind. Chem.* 1 (2017) 10–13.
- [35] C. Chen, D. Wen, J. Wang, Cellular surface characteristics of *Saccharomyces cerevisiae* before and after Ag(I) biosorption, *Bioresour. Technol.* 156 (2014), <https://doi.org/10.1016/j.biortech.2014.01.065>.
- [36] C. Can, W. Jianlong, Investigating the interaction mechanism between zinc and *Saccharomyces cerevisiae* using combined SEM-EDX and XAFS, *Appl. Microbiol. Biotechnol.* 79 (2008) 293–299, <https://doi.org/10.1007/s00253-008-1415-4>.
- [37] A. Abirami, G. Nagarani, P. Siddhuraju, Measurement of functional properties and health promoting aspects-glucose retardation index of peel, pulp and peel fiber from *Citrus hystrix* and *Citrus maxima*, *Bioact. Carbohydr. Diet. Fibre* 4 (2014), <https://doi.org/10.1016/j.bcdf.2014.06.001>.
- [38] M. Kacuráková, P. Capek, V. Sasinková, N. Wellner, A. Ebringerová, FT-IR study of plant cell wall model compounds: pectic polysaccharides and hemicelluloses, *Carbohydr. Polym.* 43 (2000), [https://doi.org/10.1016/S0144-8617\(00\)00151-X](https://doi.org/10.1016/S0144-8617(00)00151-X).
- [39] A. Fellah, P. Anjukandi, M.R. Waterland, M.A.K. Williams, Determining the degree of methylesterification of pectin by ATR/FT-IR: methodology optimisation and comparison with theoretical calculations, *Carbohydr. Polym.* 78 (2009) 847–853, <https://doi.org/10.1016/j.carbpol.2009.07.003>.
- [40] C.J. Grande, F.G. Torres, C.M. Gomez, O.P. Troncoso, J. Canet-Ferrer, J. Martínez-Pastor, Development of self-assembled bacterial cellulose-starch nanocomposites, *Mater. Sci. Eng. C* 29 (2009), <https://doi.org/10.1016/j.msec.2008.09.024>.
- [41] Z. Cai, J. Kim, Bacterial cellulose/poly(ethylene glycol) composite: characterization and first evaluation of biocompatibility, *Cellulose* 17 (2010) 83–91, <https://doi.org/10.1007/s10570-009-9362-5>.
- [42] T. Kondo, P. Rytczak, S. Bielecki, Bacterial nanocellulose characterization, in: *Bacterial Nanocellulose*, Elsevier, 2016, pp. 59–71, <https://doi.org/10.1016/B978-0-444-63458-0.00004-4>.
- [43] S. Brunauer, P.H. Emmett, E. Teller, Adsorption of gases in multimolecular layers, *J. Am. Chem. Soc.* 60 (1938), <https://doi.org/10.1021/ja01269a023>.
- [44] M. Thommes, K. Kaneko, A.V. Neimark, J.P. Olivier, F. Rodriguez-Reinoso, J. Rouquerol, K.S.W. Sing, Physisorption of gases, with special reference to the evaluation of surface area and pore size distribution (IUPAC technical report), *Pure Appl. Chem.* 87 (2015), <https://doi.org/10.1515/pac-2014-1117>.
- [45] F.D.E. Goelzer, P.C.S. Faria-Tischer, J.C. Vitorino, M.R. Sierakowski, C.A. Tischer, Production and characterization of nanospheres of bacterial cellulose from *Acetobacter xylinum* from processed rice bark, *Mater. Sci. Eng. C* 29 (2009), <https://doi.org/10.1016/j.msec.2008.10.013>.